acta physica slovaca vol. 46 No. 4, 575 – 583 August 1996

ON THE VALIDITY OF APPROXIMATION SCHEMES FOR HANBURY-BROWN/TWISS CORRELATION RADII[1]

Urs Achim Wiedemann[2], Pierre Scotto, Ulrich Heinz
Institut für Theoretische Physik, Universität Regensburg D-93040 Regensburg, FRGermany

Received 15 April 1996, accepted 13 May 1996

We have developped an analytical approximation scheme for HBT-radii which converges rapidly to the widths of the numerically computed correlation function. Higher order contributions within our approximation scheme are essential, and the previously published lowest order results with simple $m_\perp$ scaling behaviour are quantitatively and qualitatively unreliable.

1. Introduction

It is commonly agreed that the experimentally measured Hanbury-Brown/Twiss (HBT) correlations between two identical bosons of momenta p_1, p_2 should be fit to gaussians of the form[1]

$$C(\mathbf{K},\mathbf{q}) \simeq 1 + \lambda\, e^{-R_o^2(\mathbf{K})q_o^2 - R_s^2(\mathbf{K})q_s^2 - R_l^2(\mathbf{K})q_l^2 - 2R_{ol}^2(\mathbf{K})q_o q_l}, \qquad (1)$$

where $\mathbf{q} = \mathbf{p}_1 - \mathbf{p}_2$, $\mathbf{K} = \frac{1}{2}(\mathbf{p}_1 + \mathbf{p}_2)$. Here, the subscript L denotes the *longitudinal* or z-direction parallel to the beam, the *out* or x-direction parallel to the transverse component of $\mathbf{K}$ is denoted by the subscript o, and the remaining *side* or y-direction carries the subscript s.

Also, there exists a well-established[2, 3, 4] theoretical approximation for the calculation of $C(\mathbf{K},\mathbf{q})$ from specific models,

$$C(\mathbf{K},\mathbf{q}) \simeq 1 + \frac{\left|\int d^4x\, S(x,K)\, e^{iq\cdot x}\right|^2}{\left|\int d^4x\, S(x,K)\right|^2}, \qquad (2)$$

where $q^0 = E_1 - E_2$ and $K_0 = E_K = \sqrt{m^2 + |\mathbf{K}|^2}$. Here, a model is specified by an emission function $S(x,K)$ which describes the phase space density of the boson emitting source.

[1] Paper presented at the XXVth International Symposium on Multiparticle Dynamics, September 11.-16., 1995, Stara Lesna, Slovakia.
[2] E-mail address: Urs.Wiedemann@physik.uni-regensburg.de

In recent years, calculations of the momentum dependence of HBT-radii have appeared for several models $S(x,K)$.[5, 6, 1, 7] These were based on lowest order approximations in a saddle point expansion and suggest simple $m_\perp$ scaling laws. We have developped a convergent all-order approximation scheme for HBT-radii, applicable to an interesting class of emission functions, and we have checked its results against the exact values obtained numerically.[8] We find that the previously published lowest order results with simple $m_\perp$ scaling behaviour are quantitatively and qualitatively unreliable. Referring for the many technical details to the literature, we emphasize here the consequences of our findings for the physical interpretation of the measured HBT-radii.

2. HBT-radii measure the half widths of the emission function

A very popular method for calculating HBT-radii is based on the gaussian saddle point approximation[9]

$$S(x,K) \simeq S(\bar{x},K)\, e^{-\frac{1}{2}(x-\bar{x})^\mu (x-\bar{x})^\nu B_{\mu\nu}(\mathbf{K})}\,, \tag{3}$$

where $\bar{x} = \bar{x}(\mathbf{K})$ denotes the saddle point of $S(x,K)$. This leads to

$$C(\mathbf{K},\mathbf{q}) \simeq 1 + e^{-(B^{-1})_{\mu\nu} q^\mu q^\nu}\,. \tag{4}$$

Here, a technical caveat has to be made: the usual procedure[6] of determining $B_{\mu\nu}(\mathbf{K})$ via the curvature $-\partial_\mu \partial_\nu \ln S(x,K)|_{\bar{x}(\mathbf{K})}$ has a very limited range of validity and leads very often to unreliable results. In contrast, the half widths of $S(x,K)$ describe the spatio-temporal fall-off properties of realistic source distributions much better[8] since they do not presuppose a gaussian behaviour of $S(x,K)$ around the saddle point.[3] Consequently, we advocate the determination of $B_{\mu\nu}(\mathbf{K})$ via the variance of $S(x,K)$,

$$\begin{aligned} (B^{-1})_{\mu\nu} &= \langle x_\mu x_\nu \rangle - \langle x_\mu \rangle \langle x_\nu \rangle \\ \langle \xi \rangle &= \langle \xi \rangle (K) = \frac{\int d^4x\, \xi\, S(x,K)}{\int d^4x\, S(x,K)}\,, \end{aligned} \tag{5}$$

which provides a very good measure of the half widths. The HBT-radii are then given by linear combinations of the $(B^{-1})_{\mu\nu}$'s. Using the on-shell constraint of p_1, p_2, for boson pairs with $|\mathbf{q}| \ll E_K$, we can approximate the temporal component of q via $q^0 \simeq \beta_\perp q_0 + \beta_L q_L$, $\beta_i = K_i/E_K$. Inserting this into (4) and comparing to (1), one obtains for the case of an azimuthally symmetric source, (i.e. $S(x,K)$ is invariant under $y \to -y$)[1, 9, 8, 12]

$$\begin{aligned} R_s^2 &= \langle y^2 \rangle, \\ R_o^2 &= \langle (x-\beta_\perp t)^2 \rangle - \langle (x-\beta_\perp t) \rangle^2, \\ R_l^2 &= \langle (z-\beta_L t)^2 \rangle - \langle (z-\beta_L t) \rangle^2, \\ R_{lo}^2 &= \langle (x-\beta_\perp t)(z-\beta_L t) \rangle - \langle (x-\beta_\perp t) \rangle \langle (z-\beta_L t) \rangle\,. \end{aligned} \tag{6}$$

[3] E.g., an emission function $S(x,K) = e^{-\cosh x^2} g(\mathbf{K})$ has zero curvature at $\bar{x} = 0$, but is sufficiently well approximated by eqs. (3) and (5).

Let us note in passing that $(B^{-1})_{\mu\nu}$ is in general a symmetric 4×4 matrix with 10 independent entries and the mass shell constraint combines them into 6 independent HBT-radii: $R_o^2(\mathbf{K})$, $R_s^2(\mathbf{K})$, $R_l^2(\mathbf{K})$, $R_{os}^2(\mathbf{K})$, $R_{ol}^2(\mathbf{K})$, $R_{sl}^2(\mathbf{K})$. For azimuthally symmetric systems, the side-out, side-longitudinal and side-temporal elements of $(B^{-1})_{\mu\nu}$ vanish, and the remaining 7 non-zero entries combine to the 4 different HBT-radii of (6).

3. A longitudinal boost-invariant model

In what follows we study a simplified model for heavy-ion collisions which shows already a number of essential physical features.[6, 8] This model allows for a controlled investigation of our analytical approximation scheme and a direct comparison with previously published lowest order results. It is defined by the following emission function:

$$S(x,K) = \frac{m_\perp \cosh(\eta - Y)}{(2\pi)^3} e^{-\frac{K\cdot u}{T}} e^{-\frac{r^2}{2R^2}} \delta(\tau - \tau_0)\,, \tag{7}$$

where T is a constant temperature along the sharp freeze-out hypersurface $\Sigma(x) = (\tau_0 \cosh\eta, x, y, \tau_0 \sinh\eta)$, $t = \tau_0 \sinh\eta$, $z = \tau_0 \cosh\eta$, $m_\perp = \sqrt{m^2 + K_\perp^2}$, and Y is the rapidity of a particle with momentum $K_\nu = (m_\perp \cosh Y, K_\perp, 0, m_\perp \sinh Y)$. We consider a flow which shows Bjorken expansion in the longitudinal direction ($\eta = \frac{1}{2}\ln\left(\frac{t+z}{t-z}\right)$)

$$u_\nu(x) = (\cosh\eta \cosh\eta_t, \frac{x}{r}\sinh\eta_t, \frac{y}{r}\sinh\eta_t, \sinh\eta \cosh\eta_t) \tag{8}$$

with linear transverse flow profile $\eta_t(r) = \eta_f \frac{r}{R}$. The geometric extension of the source in the transverse coordinate $r = \sqrt{x^2+y^2}$ is specified by R, and η_f is the transverse flow velocity of the fluid at $r = R$.

3.1. An analytical approximation scheme

We have developped a convergent all-order approximation scheme for the HBT-radii (6) of the class of models (7). Here, we restrict ourselves to emphasizing the main points in which it differs from previous approaches, referring for further details to the literature:[8]

- the η-integration is done analytically, leading to modified Bessel functions $K_\nu(a)$, $a = \frac{m_\perp}{T}\cosh\eta_t$. In contrast, previous discussions of (7) use a gaussian saddle point approximation for the η-integration or consider the case $\eta_t(r) = 0$ only.
- The Bessel functions $K_\nu(a)$ are expanded asymptotically in a series up to order p. For each order $n \le p$, a saddle-point $\bar{x}_n(\mathbf{K})$ is determined by an interation scheme. Compared to previous discussions of the model (7), this leads to a much more accurate treatment of the x-and y-integrations.

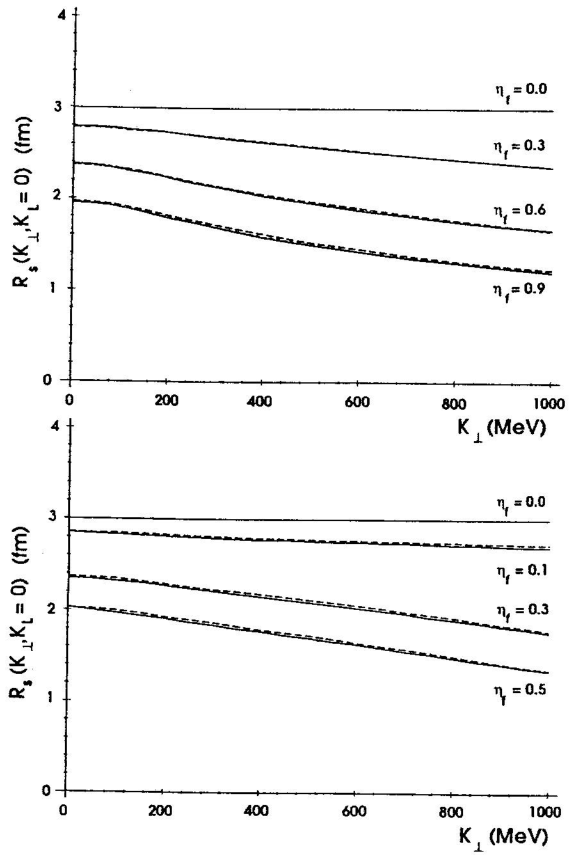

Fig. 1. The *side* HBT-radius $R_s(\mathbf{K})$ for the emission function (7) with linear (top) and quadratic (bottom) transverse flow profile.

3.2. The results

In what follows, we work in the longitudinal comoving system (LCMS) which is the longitudinal boosted Lorentz frame defined by $K_L = \beta_L = 0$. Note that the longitudinal boost invariance of $S(x, K)$ implies the symmetry of the emission function with respect to $z \to -z$ and hence, the out-longitudinal cross term $R_{ol}^2(\mathbf{K})$ vanishes for the model under consideration. To lowest order, our approximation scheme reproduces various results in the literature, as long as we insert the less accurate expressions for the saddle point $\bar{x}(\mathbf{K})$ used in these earlier discussions. Especially, we find to lowest order the old

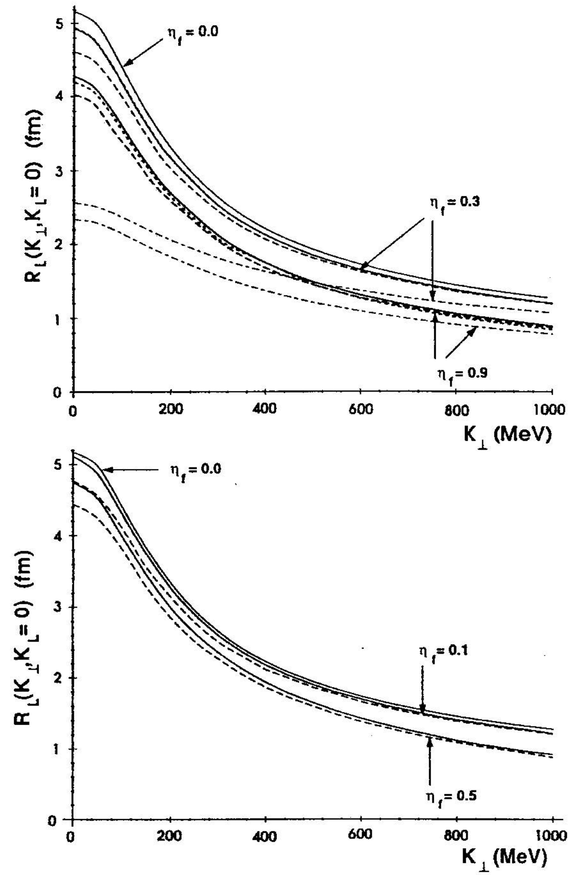

Fig. 2. The *longitudinal* HBT-radius $R_l(\mathbf{K})$ for the emission function (7) with linear (top) and quadratic (bottom) transverse flow profile.

Makhlin-Sinyukov expression

$$R_l^2 = \tau_0^2 \frac{T}{m_\perp} \qquad \text{[Makhlin and Sinyukov[5]]}, \tag{9}$$

and to next-to-lowest order, we confirm the $O(\frac{T^2}{m_\perp^2})$-part of the corrections obtained for small transverse flow $\eta_f \ll 1$:

$$R_l^2 = \tau_0^2 \frac{T}{m_\perp} \left(1 + \left(\frac{1}{2} + \frac{1}{1 + \frac{m_\perp}{T} v^2} \right) \frac{T}{m_\perp} \right), \qquad \text{[Chapman, Scotto and Heinz[1]]}, \tag{10}$$

$$\left.\begin{aligned} R_o^2 &= \frac{R^2}{1+\frac{m_\perp}{T}v^2} + \frac{1}{2}\left(\frac{T}{m_\perp}\right)^2 \beta_\perp^2 \tau_0^2 , \\ R_s^2 &= \frac{R^2}{1+\frac{m_\perp}{T}v^2} . \end{aligned}\right\} \quad \text{[Chapman, Scotto and Heinz[1]]} \qquad (11)$$

Also, for vanishing transverse flow, our calculation coincides with the exact result of Herrmann and Bertsch,

$$R_l^2 = \tau_0^2 \frac{T}{m_\perp} \frac{K_2(\frac{m_\perp}{T})}{K_1(\frac{m_\perp}{T})} \quad \text{[Herrmann and Bertsch[10]]} . \qquad (12)$$

To check the validity of these lowest order results, we have evaluated the HBT-radii for an emission function (7) with linear transverse flow according to the three different methods listed below. Also, we have evaluated numerically the HBT-radii for a quadratic transverse flow profile $\eta_t(r) = \eta_f \frac{r^2}{R^2}$. The results are compared for linear (quadratic) flow in the upper (lower) diagrams of Figs. 1 - 3:

1. The solid lines are obtained by numerical evaluation of the HBT-radii (6).
2. The long-dashed lines denote the numerically determined half width of the correlation function (2) in direction i.
3. The short-dashed lines represent the result of our analytical approximation scheme, including all terms up to order $p = 3$. The dash-dotted lines show the same analytical expressions but truncating the expansion at lowest order. These analytical results have been calculated for linear transverse flow profiles only.

Let us summarize the most important features of our results obtained for linear transverse flow [8]:

- The side radius R_s obtained analytically from (6) approximates very accurately, even to lowest order $p = 0$, the exact numerical value. Also, it is consistent with the numerically determined half width of $C(\mathbf{K},\mathbf{q})$ in (2). Our studies showed however that, if calculated with the previously used approximate expressions for the saddle point $\bar{x}(\mathbf{K})$ instead of our refined iteration scheme sketched in 3.1, R_s develops for large transverse flow rapidities $\eta_f > 0.3$ a much stronger $K_\perp$-dependence than the exact side radius. This renders an analytical determination of η_f from the $K_\perp$-dependence a somewhat subtle issue.
- For the longitudinal radius R_l, the lowest order term of the analytic approximation scheme is insufficient, but excellent agreement with the exact value of the model-independent expression (6) is reached at order $p = 3$ for all values of $K_\perp$. For small values of $K_\perp$, there is a small discrepancy between this model-independent radius and the half width of $C(\mathbf{K},\mathbf{q})$. We have checked numerically that R_l reproduces the curvature of $C(\mathbf{K}, q_l)$ at $q_l = 0$. The discrepancy can be traced back to the strong non-Gaussian behaviour of the source (7) in the η-direction. Yet, for all practical purposes, the model-independent expressions (6) are sufficiently accurate, the deviation from the half width being of the order of a few percent.

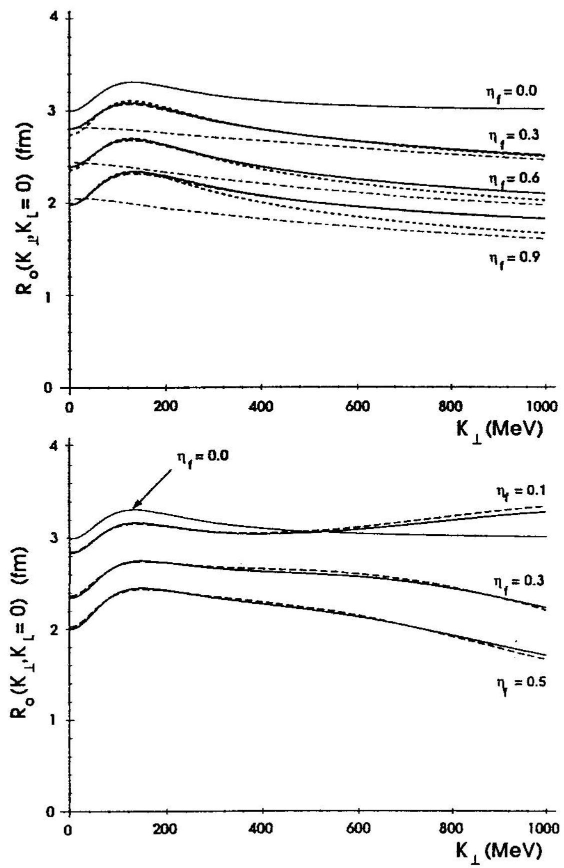

Fig. 3. The *out* HBT-radius $R_o(\mathbf{K})$ for the emission function (7) with linear (top) and quadratic (bottom) transverse flow profile.

- For the out direction, the lowest order of the analytical approximation scheme misses the qualitative behaviour completely, and qualitative as well as quantitative agreement is reached again at order $p = 3$. Also, the model-independent expression (6) agrees very accurately with the half width of the correlation function (2). The interesting increase of R_o for small $K_\perp$ is a lifetime effect which measures the time variance $\langle t^2 \rangle - \langle t \rangle^2$, being the term proportional to $\beta_\perp^2$ in equ. (6). For small transverse flows, this is the dominant contribution to the difference $R_o^2 - R_s^2$ between the out and side radii. It is non-zero even for systems with freeze-out on a sharp hypersurface since particles emitted from different points (t, z) of this surface contribute to the correlation function as long as they are seperated by less than the longitudinal region of homogeneity R_l. The correlation function probes a finite range of coordinate time, $\Delta t \simeq \sqrt{\tau_0^2 + R_l^2} - \tau_0$ along the proper time hyperbola $\tau = \tau_0$. In passing, we note that inserting the old Makhlin-Sinyukov formula (9) for R_l in this estimate of Δt, one finds $\Delta t \simeq \frac{1}{2}\tau_0\left(\frac{T}{m_\perp}\right)$. This allows us to rewrite (12) in the form $R_0^2 = R_s^2 + 2\beta_\perp^2 \Delta t^2$ which is the old lowest-order relation of Csörgő and Pratt.[11]

Let us turn to the results obtained for a quadratic flow profile $\eta_t = \eta_f \frac{r^2}{R^2}$. Again, we emphasize the main points only [8]:

- For all three radii, the model-independent expressions (6) agree very well with the corresponding half-width of the correlation function (2).
- Compared to the scenario of a linear flow profile, a given flow scale η_f leads to stronger flow effects. In general, however, this leads only to quantitative differences. The only new qualitative feature observed is the rise of R_o with $K_\perp$ for a weak quadratic flow with $\eta_f = 0.1$. This can be traced back to the rise of the variance in the out-direction, $\langle x^2 \rangle - \langle x \rangle^2$, with $K_\perp$. It is different from the generic decrease of the effective region of homogeneity with increasing $K_\perp$, and seems to be due to an accidental coincidence of parameters. It goes without saying that such a subtle qualitative change is not easy to reproduce in an approximate analytical calculation.

4. Summary

A careful analysis of the transverse momentum dependence of HBT-radii provides crucial information on the correlations between emission point x and particle momentum **K** in the source. Recently heavy ion experiments have begun to provide first quantitative information on this **K**-dependence.[12, 13] This has motivated various lowest order calculations of the HBT-radii $R_i(\mathbf{K})$ for specific models.

We have reanalyzed this issue with a combination of numerical and analytical methods. Amongst the many findings listed above, we emphasize two of very general importance:

- None of the so far suggested simple $m_\perp$ scaling laws is quantitatively reliable, except for very limited regions of parameter space which are not likely to be established in experiments.
- For all practical purposes, the model-independent expressions for the HBT-radii (6) allow for a very accurate determination of the half widths of $C(\mathbf{K}, \mathbf{q})$. They turn out to be the most appropriate starting point for both numerical and analytical calculations of HBT-radii.

In our work, we have developped in the context of simple models the analytical and numerical tools for an accurate calculation of the momentum dependence of HBT-radii. Our next step is to use this well-defined starting point for the treatment of more complicated models (e.g. models including resonance decays) and their comparison with experiment.

Acknowledgements This work was supported by BMBF and DFG.

References

[1] S. Chapman, P. Scotto, U. Heinz: *Phys. Rev. Lett.* **74** (1995) 4400 ; *Heavy Ion Physics* **1** (1995) 1.
[2] S. Pratt, T. Csörgő, J. Zimányi: *Phys. Rev. C* **42** (1990) 2646
[3] E. Shuryak: *Phys. Lett. B* **44** (1973) 387 ; *Sov. J. Nucl. Phys.* **18** (1974) 667.
[4] S. Chapman, U. Heinz: *Phys. Lett. B* **340** (1994) 250
[5] A.N. Makhlin, Y.M. Sinyukov: *Z. Phys. C* **39** (1988) 69
[6] Y.M. Sinyukov: in *Hot Hadronic Matter: Theory and Experiment*, p. 309, edited by J. Letessier et al. (Plenum, New York, 1995); S.V. Akkelin, Y.M. Sinyukov: *Bogolyubov Institute for Theoretical Physics, Preprint ITP-63-94E, Phys. Lett. B*, in press.
[7] T. Csörgő, B. Lörstad: *Los Alamos e-print archive hep-ph/9509213*
[8] U.A. Wiedemann, P. Scotto, U. Heinz: *Phys. Rev. C* **53** (1996) 918
[9] S. Chapman, J.R. Nix, U. Heinz: *Phys. Rev. C* **52** (1995) 2694
[10] M.Herrmann, G.F.Bertsch: *Phys. Rev. C* **51** (1995) 328
[11] T. Csörgő, S. Pratt: in *Proceedings of the workshop on relativistic heavy ion physics*, p. 75, edited by T. Csörgő e.al., Preprint KFKI-1991-28/A.
[12] NA35 Coll., T. Alber et al.: *Z.Phys.* **C66** (1995) 77 ; T. Alber et al.: *Phys. Rev. Lett.* **74** (1995) 1303
[13] NA44 Coll., H. Beker et al.: *Phys. Rev. Lett.* **74** (1995) 3340